

## Photoinitiated Reactions of 2,4,6 TCP on Degussa P25 Formulation TiO<sub>2</sub>: Wavelength-Sensitive Decomposition

Deanna C. Hurum,<sup>†</sup> Kimberly A. Gray,<sup>\*,†</sup> Tijana Rajh,<sup>‡</sup> and Marion C. Thurnauer<sup>\*,‡</sup>

*Institute for Environmental Catalysis and Department of Civil and Environmental Engineering, Northwestern University, Evanston, Illinois and Chemistry Division, Argonne National Laboratory, Argonne, Illinois 60439*

*Received: July 1, 2004*

The photoinitiated oxidative reactions of 2,4,6 trichlorophenol (2,4,6 TCP) and 2,4,5 trichlorophenol (2,4,5 TCP) are studied on the titania photocatalyst Degussa P25. On this catalyst 2,4,6 TCP is used to confirm two distinct oxidative mechanisms that are triggered at different light-excitation wavelengths. A charge-transfer mechanism occurs at sub-bandgap energies of the photocatalyst leading to a phenoxyl radical product and an oxidative mechanism occurs at the bandgap leading to a semiquinone radical product. The wavelength dependence of these two mechanisms is discussed.

### Introduction

To improve photocatalytically promoted oxidative chemistry of organic compounds, it is important to understand the mechanisms of the photoinitiated reactions. Photocatalytic systems can rapidly degrade organic pollutants, ideally mineralizing them to carbon dioxide. However, as with many radical mediated reactions, numerous degradation pathways are possible. Some of these pathways do not lead to compounds that favor mineralization, instead leading to unwanted decomposition products. In certain cases these pathways can instead be employed for synthetic purposes.<sup>1–4</sup> A wide variety of techniques has been used to elucidate the oxidation pathways of chlorinated organic compounds. Often, these methods rely on the organic compound or its products being in a homogeneous solution.<sup>5,6</sup> Thus, they provide significant insight into transient intermediates and stable byproducts, but the radical reactions characteristic of heterogeneous catalytic surfaces are more difficult to probe. Such catalytic surfaces may promote the same chemistry, but lead to altered kinetics and product ratios. In practical applications, semiconductor catalysts are heterogeneous in nature and surface reactions are of great interest. Characterization of these surface reactions is critical to understanding the mechanisms and the reaction products.

Titania is frequently used as a photocatalyst in gas and aqueous phases, as well as in solid-state such as in consumer products (e.g., self-cleaning glass and air purifiers).<sup>7,8</sup> The widespread use of TiO<sub>2</sub> can, in large part, be attributed to the convenience of a bandgap in the near-UV that spans the redox properties of water.<sup>9,10</sup> Upon illumination with photons having energy greater than the bandgap an electron is excited from the valence band to the conduction band, resulting in a photo-generated hole in the valence band and an electron in the conduction band. If these charges do not recombine, they are capable of oxidation and reduction, respectively. The ability of TiO<sub>2</sub> to photocatalyze the hydrolysis of water at near-visible wavelengths of light makes it useful for many applications as a producer of strongly oxidizing radicals, similar to hydroxyl radicals, originating from the photogenerated holes. Unfortu-

nately, these oxidizing radicals are indiscriminant, leaving few options for controlling the oxidative chemistry. While much research has been carried out to investigate the role of pH, O<sub>2</sub>, temperature, and catalyst loadings,<sup>11–14</sup> controlling selectivity of the catalyst remains difficult. If selective control of chemical mechanisms can be achieved, the potential uses for titania catalysts greatly increase.<sup>15</sup>

Degussa P25 is a commonly used formulation of TiO<sub>2</sub>, consisting of a mixture of anatase (bandgap = 385 nm) and rutile (bandgap = 410 nm) mineral phases. This formulation has been found to be particularly active at oxidizing organic compounds and is frequently used as a representative mixed-phase titania catalyst. Previous work has suggested that the products formed from the photocatalytic reaction of organic compounds with Degussa P25 are sensitive to the wavelength of illumination of the catalyst. Most of these studies focus primarily on light energies greater than the anatase bandgap in the near UV (<385 nm).<sup>16,17</sup> Recent studies have also reported photoreaction under sub-bandgap illumination conditions. Since these studies were performed on Degussa P25, their findings are specific to mixed-phase titania catalysts. It has been shown that sub-bandgap irradiation can promote chemistry on Degussa P25 that does not occur when pure-phase anatase or rutile are used.<sup>1,4,18</sup> Furthermore, mixed-phase titania catalysts have been shown to have greater photoactivity than single-phase catalysts. Recent work indicates that in P25 rutile acts as an antenna, extending the range of bandgap excitation in the visible up to 410 nm. Furthermore, electron transfer from rutile to anatase produces stabilized charge separation and increased efficiency.<sup>18</sup> The purpose of this research is to explore the wavelength dependence of surface reactions on a mixed-phase titania catalyst (Degussa P25).

Chlorophenolic reactions on TiO<sub>2</sub> under UV illumination have been well studied with the most common initial products being quinones and catechols.<sup>19,20</sup> The principal products formed by hole attack on the ring may or may not lead to dechlorination depending on the positions of the chlorine atoms, indicating differences in the preferred point of radical ion attack. The mechanism of chlorophenol oxidative dechlorination is generally thought to be electrophilic substitution of the hole on the ring, followed by eventual chloride release.<sup>21–25</sup> In this work, Electron Paramagnetic Resonance (EPR) is used to study the effect of illumination wavelength on the oxidation products of model

\* To whom correspondence should be addressed. E-mail: k-gray@northwestern.edu, MarionT@anl.gov.

<sup>†</sup> Northwestern University.

<sup>‡</sup> Argonne National Laboratory.

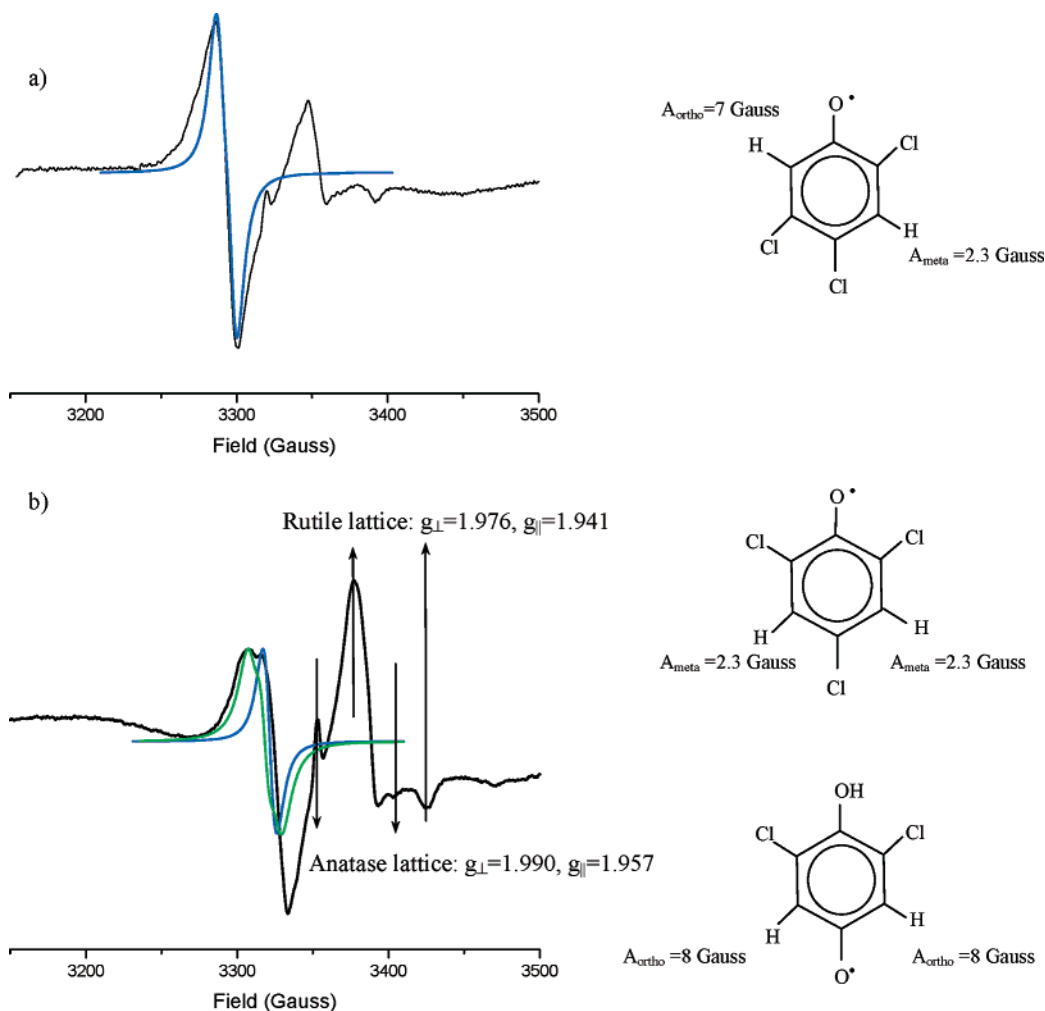


**Figure 1.** (a) Spectrum of 2,4,5 TCP on Degussa P25 under UV illumination and simulation (blue) of the TCP phenoxyl radical. Simulation hyperfine couplings: 2.3 G ( $a_{\text{H meta}}$ ), 7 G ( $a_{\text{H ortho}}$ ). The shoulders that are not simulated indicate the presence of a second product. (b) Spectrum of 2,4,6 TCP on Degussa P25 under UV illumination. Two products are clearly visible. The blue line is the simulation of the phenoxyl radical. ( $a_{\text{H meta}} = 2.3$  G) The green line is the simulation of the semiquinone radical. ( $a_{\text{H ortho}} = 8$  G) Catechol radicals would fall within the line width of the phenoxyl radical and cannot be confirmed or ruled out.

organic compounds on Degussa P25. The trichlorophenols 2,4,5 trichlorophenol (2,4,5 TCP) and 2,4,6 trichlorophenol (2,4,6 TCP) were used due to their environmental impact as common recalcitrant chlorinated contaminants and as suitable models for a large class of pollutants that includes chlorinated aromatic chemicals. Additionally, 2,4,6 TCP was chosen as a model for its high symmetry and similar chemistry to simplify spectral interpretation. EPR allows for detection and identification of radicals to directly probe the radical reactions of these compounds on  $\text{TiO}_2$  surfaces.

At low temperatures, such as 10 K, the initial products from photoinitiated reactions are trapped. By conducting low-temperature EPR experiments while illuminating a TCP/ $\text{TiO}_2$  sample, TCP reactions on  $\text{TiO}_2$  are studied. Diffusion is significantly limited in these frozen samples, allowing trapping of the products of reactions between the adsorbed TCP and the photogenerated charged species on  $\text{TiO}_2$ . In addition to the organic radicals, the electron-trapping sites in the  $\text{TiO}_2$  lattice are also probed, providing further details of the reaction mechanisms.

## Materials and Methods

Degussa P25 was kindly donated by Degussa: Huls Corporation. Samples of a titania slurry (40 g/L) of Degussa P25

were prepared in either 18 M $\Omega$  water (MilliQ) or a solution of 0.8 mM 2,4,6 TCP (aqueous) (Aldrich) as previously described.<sup>18</sup> Immediately following preparation of these slurries, they were degassed by nitrogen purge, transferred under nitrogen atmosphere to 3 mm quartz tubes, and frozen in liquid nitrogen to form a water glass.

EPR spectra were collected on a Varian E-9 spectrometer equipped with a helium cryostat. Samples were cooled to 10 K and illuminated within the cavity at that temperature while spectra were acquired. A 300-W xenon lamp (ILC Inc.) was used. Illumination while taking spectra was continuous and typically lasted for 30 min. For wavelength-controlled experiments, long-pass filters (Schott) of the appropriate wavelength were used. Prior to illumination, samples were monitored for any dark background signals, as was the microwave cavity both before and after illumination. Simulation of EPR spectra was performed using Bruker's SimFonia simulation package.

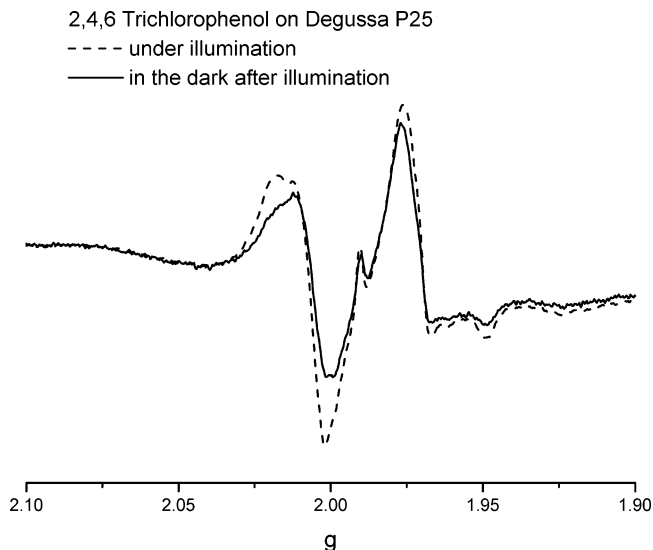
## Results and Discussion

Figure 1 shows the EPR spectra obtained from both 2,4,5 TCP and 2,4,6 TCP on Degussa P25 under illumination ( $\lambda > 380$  nm) at 10 K. In these spectra the clear signature of organic radicals is present at  $g = 2.004$ . In addition to this organic radical signal, signals from trapped electrons are assigned to

lattice electron-trapping sites in anatase. The remaining signals at  $g_{\perp} = 1.976$  and  $g_{\parallel} = 1.941$  are the lattice electron-trapping sites in rutile. Phenoxyl radicals have been previously identified as initial photocatalytic products by pulse radiolysis.<sup>26</sup> The signal seen in Figure 1a resulting from illuminating 2,4,5 TCP on TiO<sub>2</sub> can be simulated using  $g$  values of 2.004 ( $g_x$ ) and 2.0025 ( $g_y$ ,  $g_z$ ) and the hydrogen hyperfine constants of 7 G ( $a_{\text{H ortho}}$ ) and 2.3 G ( $a_{\text{H meta}}$ ) previously found for the phenoxyl radical.<sup>27</sup> The production of phenoxyl radicals is in agreement with the pulse radiolysis data. Unfortunately, due to low substitutional symmetry of 2,4,5 TCP the width of the signal obscures clear observation of other potential products. However, the small shoulders that are not accounted for by the simulation of the phenoxyl radical are an indication of a possible secondary mechanism for radical generation. Unlike the spectrum of 2,4,5 TCP on TiO<sub>2</sub>, the spectrum of 2,4,6 TCP in Figure 1b clearly shows two radical products (resonances around  $g = 2$ ) with a relative intensity that is approximately 1.1 (low field signal):1. The narrower signal observed at  $g = 2.004$  is consistent with that of a signal from a phenoxyl radical with hyperfine couplings of 2.3 G from the two equivalent protons in the meta position.<sup>28</sup> A simulated spectrum of the phenoxyl radical using  $g$  values of 2.004 ( $g_x$ ), and 2.0025 ( $g_y$ ,  $g_z$ ) and proton hyperfine couplings of 2.3 G ( $a_{\text{H meta}}$ ) is shown in Figure 1. This simulation closely matches the first peak at  $g = 2.004$ . The symmetric substitution of the chlorine atoms in 2,4,6 TCP leads to a narrower signal for the phenoxyl radical compared to that from 2,4,5 TCP, and this increase in resolution allows for the observation of a second radical product.

The second signal visible in the spectrum in Figure 1b has a larger hyperfine coupling compared to the phenoxyl radical as indicated by its broader overall line shape in the EPR spectrum. With the 2,4,6 TCP isomer, the only process that would allow a large coupling to be observed is radical attack at a chlorinated position. Dechlorination by such an attack has been observed previously and these results provide further evidence that such a process occurs.<sup>24</sup> Two products are possible by dechlorination. Either a semiquinone-type or a catachol-type radical could form. EPR experiments on semiquinone radicals predict that the solution hyperfine coupling of the protons for a similar radical are 5.6 G ( $a_{\text{H ortho}}$ ), leading to a spectrum that is much broader than that of the 2,4,6 TCP phenoxyl radical.<sup>29</sup> This greater hyperfine coupling would be consistent with the data and simulations in Figure 1b, simulated with *ortho* hydrogen couplings of 8 G. A slight increase in hyperfine coupling is not unusual for species adsorbed to semiconductor surfaces and a 7–8 G coupling is common for *ortho* hydrogen atoms in phenolic radicals. This semiquinone product has also been shown to be the preferred product of 2,4,6 TCP oxidation on Degussa P25 in other studies.<sup>21</sup> Comparatively, attack at either of the *ortho*-position chlorine atoms to form a catachol product would lead to a radical with couplings of only 3.8 G.<sup>30</sup> Such a reaction may take place, but the spectrum of the resulting radical would easily be masked by the spectrum of the phenoxyl radical and would not be the source of the observed second signal.

Figure 2 shows the evolution of the two different radical species after illumination is ceased. The signal from the dechlorination product decreases markedly compared to that of the phenoxyl radical with a relative intensity of approximately 0.7 (low field signal):1. This difference in stability in the dark after illumination illustrates two points. The two signals observed are from two independent radical species. There is no evidence for conversion between the two species at these temperatures, indicating that the radical transients evolve



**Figure 2.** Spectra of 2,4,6 TCP on Degussa P25 under illumination and in the dark after illumination. The signal attributed to semiquinone radicals reacts in the dark at 10 K to form diamagnetic products leaving a greater fraction of the phenoxyl radical.

independently through separate surface reactions. This spectrum also indicates the greater stability of the phenoxyl radical with respect to the semiquinone radical, which in this system is apparently transformed at 10 K into stable nonparamagnetic products in the dark.

To investigate the different mechanisms of radical generation, wavelength-controlled experiments were performed. Figure 3 shows the EPR spectra obtained when slurries of Degussa P25 (a) and 2,4,6 TCP/Degussa P25 (b) are illuminated with light of increasing energy. The top pair of spectra result from illumination using a 460-nm long-pass filter. Illumination with these wavelengths does not lead to significant charge separation in either anatase or rutile, as shown in Figure 3a. Comparatively, in Figure 3b a signal characteristic of organic phenoxyl radicals at  $g = 2.004$  is present. Additionally, weak signals from both anatase and rutile electron lattice-trapping sites are observed. Similarly, when illuminated using a 422-nm long-pass filter, there is still no significant charge separation on P25, yet the phenoxyl radical signal increases in intensity, as do the lattice electron trapping site signals in the TCP/P25 sample. The lack of charge separation in the TiO<sub>2</sub> slurry at sub-bandgap energies in these experiments indicates that the radical observed in the TCP/TiO<sub>2</sub> sample is not due to bandgap excitation of the catalyst. Instead, we suggest that a previously observed charge-transfer complex between the catalyst and the TCP<sup>1,4,31</sup> leads to the production of the phenoxyl radical. In this case, an electron is donated from TCP to the catalyst, populating the lattice trapping sites of both the anatase and rutile phases, leaving the phenoxyl radical of TCP on the surface. This charge-transfer complex with TiO<sub>2</sub> has been confirmed by diffuse reflectance UV–vis for both the 2,4,6 TCP and 2,4,5 TCP isomers. The broad charge-transfer band extends well into the visible, with a  $\lambda_{\text{max}} = 420$  nm leading to photochemistry that occurs at much lower energy than the traditional bandgap chemistry. For comparison, the maximum UV–vis absorption of 2,4,6 TCP occurs at 290 nm. Similar observations of a charge transfer complex have been noted previously with 4-chlorophenol.<sup>6,11</sup> While at sub-bandgap energies, as the wavelength of illumination decreases, both the organic radical signal and the lattice electron-trapping site signals continue to increase, indicating further electron transfer to the catalyst from TCP.

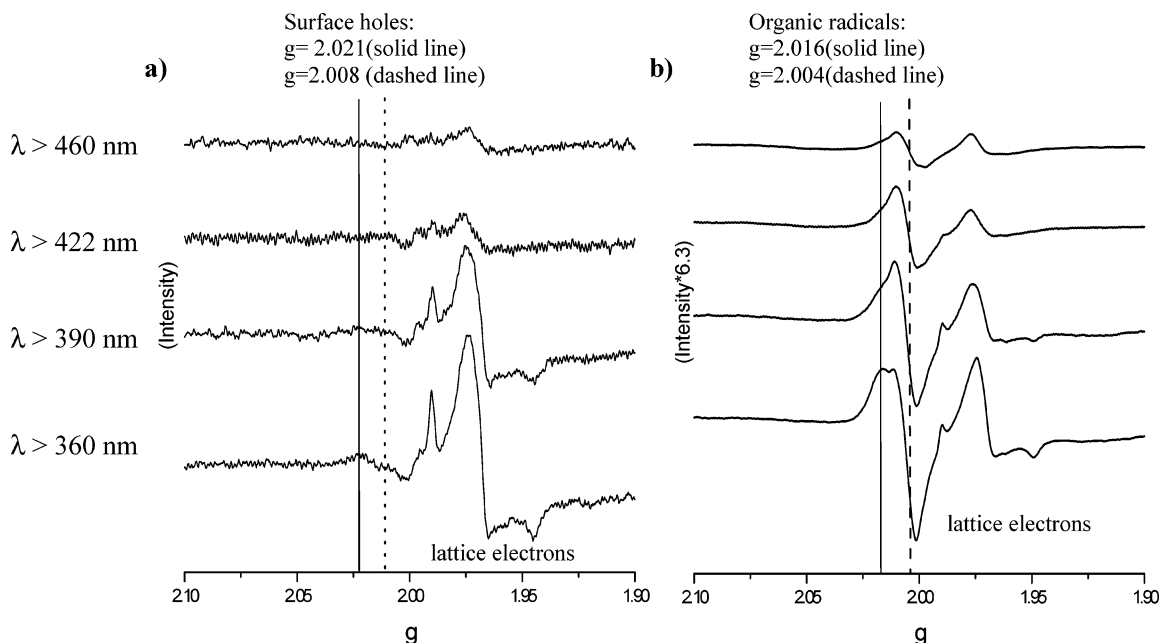


**Figure 3.** EPR spectra Degussa P25 in water and of 2,4,6 TCP adsorbed on Degussa P25 at increasing wavelengths of light. Note the appearance of lattice electrons at wavelengths not capable of band-gap excitation. The spectra obtained from 2,4,6 TCP on Degussa P25 are 6.3 times more intense than those obtained from Degussa P25 in water. Each spectrum has been corrected for the cavity background.

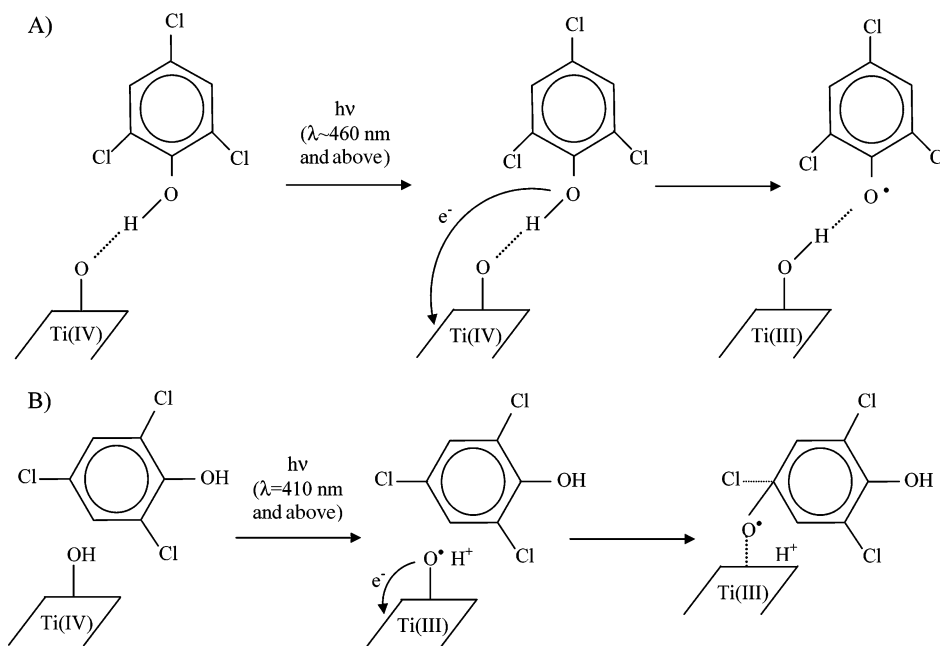


**Figure 4.** Two proposed mechanisms of trichlorophenol oxidation on  $\text{TiO}_2$  with different wavelengths of light. (A) Charge-transfer complex mechanism leading to phenoxyl radicals at light of energy well below  $\text{TiO}_2$  bandgap energies. (B) Oxidation leading to eventual dechlorination by surface holes formed by bandgap electron transfer within  $\text{TiO}_2$ .

When the rutile bandgap is excited (390 nm), both the TCP/ $\text{TiO}_2$  and the  $\text{TiO}_2$  samples show charge separation. The TCP/ $\text{TiO}_2$  slurry shows a strongly enhanced lattice electron-trapping site signal, and the signal from the semiquinone radical product becomes significant. In the  $\text{TiO}_2$  slurry, weak hole signals and lattice electron signals are present. This wavelength of light can generate charge separation on rutile. Furthermore, the holes generated are capable of oxidizing TCP, forming the dechlorination semiquinone product, marked at  $g = 2.016$  in Figure 3b. When the anatase bandgap is exceeded at 360 nm, the second TCP radical product is clearly enhanced. In this case, both anatase and rutile bandgaps are stimulated, leading to greater oxidation. The continued presence of trapped lattice and surface

electrons indicates no initial reaction of the electrons with the TCP or the oxidation products that are formed.

These data demonstrate that there are two distinct and concurrent processes occurring on the surface of the  $\text{TiO}_2$  catalyst under bandgap illumination: the electron transfer from the phenol to the catalyst leading to a phenoxyl radical and a second oxidation process leading to attack at the para position by the surface bound holes (Figure 4). As has been noted elsewhere, the charge-transfer behavior does not occur on pure-phase anatase or rutile.<sup>1</sup> The lack of a charge-transfer complex on pure-phase materials indicates the existence of a surface structure on the mixed-phase material that enhances the phenol–titania complex. We propose that the unique morphology of



Degussa P25, the structure of which is an active area of debate,<sup>32–34</sup> leads to a distorted defect site where the formation of a charge transfer complex is favorable. Such a site is likely to occur at the interface of the anatase and rutile particles where other processes, such as phase transformation, have been shown to be enhanced.<sup>32</sup> This site, in addition to adsorption sites on undistorted anatase and rutile single crystal-like surfaces, likely leads to the two observed mechanisms of oxidation.

## Conclusions

The two trichlorophenols studied exhibit two primary oxidative radical pathways: one a photoinduced charge transfer product, the other a photocatalytic oxidation product. While both phenols undergo these pathways, the 2,4,6 TCP isomer was used to clarify the behavior. These two pathways are active at different wavelengths, leading to wavelength dependence in the products produced. Such wavelength dependence has great potential in controlling the chemistry of an ordinarily nonselective oxidizing catalyst.

**Acknowledgment.** The authors thank Degussa:Hulls for their generous donation of P25. This work was supported by the Northwestern University Institute for Environmental Catalysis (IEC), funded through a grant from the National Science Foundation (NSF) with matching funds from Northwestern University and the U.S. Department of Energy (CHE-9810378). IEC work at Argonne National Laboratory was supported by the U.S. Department of Energy, Office of Basic Energy Sciences, Division of Chemical Sciences, under contract W-31-109-Eng-38.

## References and Notes

- (1) Agrios, A. G.; Gray, K. A.; Weitz, E. *Langmuir* **2003**, *19*, 1402.
- (2) Schoumacker, K. et al. *J. Photochem. Photobiol. A* **2002**, *152*, 147.

- (3) Lin, C. H. et al. *Catal. Lett.* **2001**, *73*, 121.
- (4) Agrios, A. G.; Gray, K. A.; Weitz, E. *Langmuir* **2004**, *20*, 5911.
- (5) Burrows, H. D. et al. *Prog. React. Kinet.* **1998**, *43*, 45.
- (6) Stafford, U.; Gray, K. A.; Kamat, P. V. *J. Phys. Chem.* **1994**, *98*, 6343.
- (7) Romeas, V. et al. *New J. Chem.* **1999**, *23*, 365.
- (8) Pichat, P. et al. *Catal. Today* **2000**, *63*, 363.
- (9) Linsebigler, A. L.; Lu, G.; Yates, J. T. *Chem. Rev.* **1995**, *95*, 735.
- (10) Hoffmann, M. R.; Martin, S. T.; Choe, W.; Bahnemann, D. W. *Chem. Rev.* **1995**, *95*, 69.
- (11) Stafford, U.; Gray, K. A.; Kamat, P. V. *J. Catal.* **1997**, *167*, 25.
- (12) Stafford, U.; Gray, K. A.; Kamat, P. V. *Heterogeneous Chem. Rev.* **1996**, *3*, 77.
- (13) Theurich, J.; Lindner, M.; Bahnemann, D. W. *Langmuir* **1996**, *12*, 6368.
- (14) Richard, C.; Bosquet, F.; Pilichowski, J.-F. *J. Photochem. Photobiol., A* **1997**, *108*, 45.
- (15) Agrios, A. G.; Gray, K. A. In *Environmental Catalysis*; Grassens, V. H. Ed.; Marcel Dekker: New York, 2004; in press.
- (16) Emeline, A.; Serpone, N. *J. Phys. Chem. B* **2002**, *106*, 12221.
- (17) Emeline, A. et al. *J. Photochem. Photobiol., A* **2002**, *148*, 97.
- (18) Hurum, D. C. et al. *J. Phys. Chem. B* **2003**, *107*, 4545.
- (19) Burrows, H. D. et al. *Prog. React. Kinet.* **1998**, *23*, 145.
- (20) Stafford, U.; Gray, K. A.; Kamat, P. V. *Res. Chem. Intermed.* **1994**, *20*, 835.
- (21) D'Olivera, J.-C. et al. *J. Photochem. Photobiol., A* **1993**, *72*, 261.
- (22) Antonaraki, S. et al. *J. Photochem. Photobiol., A* **2002**, *148*, 191.
- (23) Skurlatov, Y. I. et al. *J. Photochem. Photobiol., A* **1997**, *107*, 207.
- (24) Mills, G.; Hoffmann, M. R. *Environ. Sci. Technol.* **1993**, *27*, 1681.
- (25) Vinodgopal, K.; Stafford, U.; Gray, K. A.; Kamat, P. V. *J. Phys. Chem.* **1994**, *98*, 6797.
- (26) Draper, R. B., et al. *J. Phys. Chem.* **1989**, *93*, 1938.
- (27) Dixon, W. T.; Murphy, D. J. *Chem. Soc., Faraday Trans. 2* **1976**, *72*, 1221.
- (28) Shiga, T.; Imaizumi, K. *Arch. Biochem. Biophys.* **1973**, *154*, 540.
- (29) Meng, Q. X.; Hayashi, H. *Mol. Phys.* **1995**, *85*, 363.
- (30) Reszka, K.; Lown, J. W.; Chignell, C. F. *Photochem. Photobiol.* **1992**, *55*, 359.
- (31) Agrios, A. G. Visible Light Photocatalysis: Adsorption, Complexation, and Reaction of Chlorophenols on Titania. Ph.D. Thesis, Northwestern University, Evanston, IL. April 2003.
- (32) Penn, R. L.; Banfield, J. F. *Am. Mineral.* **1999**, *84*, 871.
- (33) Datye, A. K. et al., *J. Solid State Chem.* **1995**, *115*, 236.
- (34) Bickley, R. I. et al., *J. Solid State Chem.* **1991**, *92*, 178.